PHYSICAL REVIEW B **80**, 081413(R) (2009)

# Thermopower and Nernst effect in graphene in a magnetic field

Joseph G. Checkelsky and N. P. Ong
*Department of Physics, Princeton University, Princeton, New Jersey 08544, USA*

(Received 13 January 2009; revised manuscript received 2 August 2009; published 27 August 2009)

We report measurements of the thermopower $S$ and Nernst signal $S_{yx}$ in graphene in a magnetic field $H$. Both quantities show strong quantum oscillations vs the gate voltage $V_g$. Our measurements for Landau levels of index $n \neq 0$ are in quantitative agreement with the edge-current model of Girvin and Jonson (GJ). The inferred off-diagonal thermoelectric conductivity $\alpha_{xy}$ is consistent in magnitude with GJ's prediction. At the Dirac point ($n=0$), however, the width of the peak in $\alpha_{xy}$ is very narrow. We discuss the physical meaning of the peak width and the puzzle raised by $\alpha_{xy}$ for states at the Dirac point.

DOI: 10.1103/PhysRevB.80.081413 PACS number(s): 73.63.Bd, 72.15.Jf, 73.43.Fj

In graphene, the electronic states at the corners $K$ and $K'$ of the first Brillouin zone have a linear dispersion described by the two-dimensional (2D) massless Dirac Hamiltonian. In a magnetic field $\mathbf{H}$, graphene exhibits the integer quantum Hall effect (QHE).[1–4] As the chemical potential $\mu$ is raised, successive filling of Landau levels (LLs) leads to a Hall conductivity that is quantized as $\sigma_{xy}=(4e^2/h)[n+\frac{1}{2}]$, where $e$ is the electron charge, $h$ is Planck's constant, and $n$ is the Landau-level index. The QHE in graphene exhibits novel features not encountered in quadratic systems based on GaAs, especially in the $n=0$ LL. To date, these issues have been explored nearly exclusively by resistance measurements.[1–7] By contrast, the thermoelectric response is much less investigated. An applied temperature gradient $-\nabla T \| \hat{\mathbf{x}}$ (with $\mathbf{H} \| \hat{\mathbf{z}}$) generates an electric field $\mathbf{E}$ in the sample with components $E_x=S_{xx}(-\partial_x T)$ and $E_y=S_{yx}(-\partial_x T)$, where $S_{ij}$ is the thermopower tensor. A thermopower measurement yields $E_x$ (hence $S_{xx}$), while the Nernst effect yields $E_y$ and $S_{yx}$. By measuring the elements of $S_{ij}$ and $\sigma_{ij}$ (the conductivity tensor), we may determine the charge current density $\mathbf{J}$ produced by $-\nabla T$. Its transverse component $J_y$ is especially interesting in the QHE regime. According to Girvin and Jonson (GJ),[8,9] the ratio $J_y/|\nabla T|$ has the quantized value $(k_B e/h)\ln 2$ when $n \neq 0$ ($k_B$ is Boltzmann's constant). However, nothing is known about how $J_y$ behaves in the $n=0$ LL (where the GJ theory fails). We investigate this little-explored quantization in graphene. [For later reference, $J_y$ is given by $J_y=\alpha_{yx}(-\nabla T)$, where the thermoelectric conductivity tensor $\alpha_{ij}$ relates $-\nabla T$ to $\mathbf{J}$.]

A most unusual feature of the thermoelectric response of a QHE system is that the thermopower displays a large peak at each LL ($n \neq 0$), whereas the Nernst signal is small. In the geometry treated by GJ (Refs. 8 and 9) [Fig. 1(a)], the 2D sample is of finite width along $\hat{\mathbf{x}}$ but is infinite along $\hat{\mathbf{y}}$. As we approach either edge, the energy $E_n(x)$ of each LL rises very steeply (bold curve). At $T=0$, edge currents $I_y$ exist at the intersections of $E_n$ with the chemical potential $\mu$ (open circles). In a gradient $-\nabla T$, the magnitude of $I_y$ is larger at the warmer edge compared with the cooler edge because of increased occupation of states above $\mu$. As we show below, the current difference $\delta I_y$ is quantized. For a finite sample, $\delta I_y$ produces a quantized Hall potential $V_H=(h/e^2)\delta I_y$ whose gradient lies $\|(-\nabla T)$. Consequently, when $\mu$ is aligned with the LL energy in the bulk $E_n$, $S_{xx} \sim E_x$ displays a large peak, whereas the Nernst signal $S_{yx} \sim E_y$ is small.

As mentioned, the calculation of GJ does not extend to the $n=0$ LL. Moreover, the nature of the edge currents at $n=0$ (Dirac point in graphene) is the subject of current debate.[6,7,10–13] What are the profiles of $S$ and $S_{yx}$? We have measured $S_{ij}$ and $R_{ij}$ to a maximum $H$ of 14 T at 20 and 50 K. Our results reveal that, at 9 T, the thermoelectric response in graphene already falls in the quantum regime at 50 K. The inferred off-diagonal term $\alpha_{xy}$ is a series of peaks independent of $n$, $B$, and $T$. The peak values are compared with $(k_B e/h)\ln 2$ below.

To measure the thermopower, we used a technique developed by Kim's group for carbon nanotubes.[14] The graphene sample was exfoliated onto a thin layer (300 nm) of $SiO_2$ grown on $n$-doped Si wafer. A strip of gold evaporated near one end of the sample served as the heat source [labeled "Heater" in Fig. 1(d)]. To measure the gradient $-\nabla T$, we evaporated the two gold strips labeled "Therm1" and "Therm2." Their four-probe resistances were measured to four significant figures between 10 and 300 K. Thereafter, they could be employed as resistance thermometers for sensing the local temperature at the two ends (with resolution $\sim \pm 1$ mK above 10 K). They were also used as current leads for measurements of $R_{ij}$. The voltage signals $V_{ij}$ were detected by the four gold lines labeled as "Signal Leads." For a temperature difference $\delta T \sim 10$ mK, the uncertainty in the gradient $-\nabla T$ was $\pm 10\%$, mostly due to the uncertainty in the voltage lead spacing ($\sim 2$ $\mu$m). To improve the signal-to-noise ratio, we used an alternating heater current of frequency $\omega/2\pi \sim 3$ Hz to produce an alternating gradient. The thermoelectric response was detected at $2\omega$, with a phase shift of $-90°$.

In our geometry with $-\nabla T \| \hat{\mathbf{x}}$, $\mathbf{H} \| \hat{\mathbf{z}}$, the charge current density $\mathbf{J}$ is $J_i=\Sigma_j[\sigma_{ij}E_j+\alpha_{ij}(-\partial_j T)]$ $(i=x,y)$. Setting $\mathbf{J}=0$, we solve for $\mathbf{E}$ and obtain

$$E_i = -\sum_{k,j} \rho_{ik}\alpha_{kj}(-\partial_j T) = \sum_j S_{ij}(-\partial_j T), \tag{1}$$

with $\rho_{ij}=R_{ij}$ the 2D resistivity tensor. The thermopower $S=-E_x/|\nabla T|$ equals $\rho_{xx}\alpha_{xx}+\rho_{yx}\alpha_{xy}$ ($S>0$ for hole doping), while the Nernst signal is given by $S_{yx}=\rho_{xx}\alpha_{xy}-\rho_{yx}\alpha_{xx}$ (with $\rho_{xx}=\rho_{yy}$).

Inverting Eq. (1), we may calculate the tensor $\alpha_{ij}$ from measured quantities. We have

 

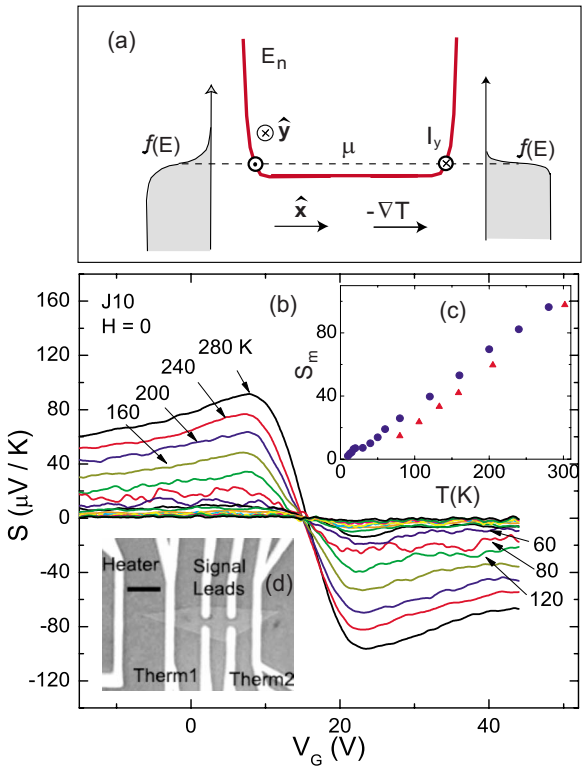


FIG. 1. (Color online) (a) The effect of $-\nabla T$ on the edge currents $I_y$ in a QHE system ($n \neq 0$). The energy $E_n$ of a LL (bold curve) increases very steeply at the sample edges. The dashed line is the chemical potential $\mu$. If $H_z > 0$, $I_y$ is negative (positive) at the left (right) edge as indicated by open circles. The magnitude $|I_y|$ is larger at the warmer edge. Fermi-Dirac distributions $f(E)$ are sketched at the sides. (b) Curves of thermopower $S = -S_{xx}$ vs gate voltage $V_g$ in sample J10 at selected $T$. The curves are antisymmetric about the Dirac point which occurs at the offset voltage $V_0 = 15.5$ V. The peak value $S_m$ is nominally linear in $T$ from 25 to 300 K (c). Less complete data from sample K59 are also plotted. A photo of sample J10 (faint polygon) is shown in (d). A microheater as well as thermometers (therm) and signal leads are patterned with electron-beam lithography. The black scale bar is 3 $\mu$m.

$$\alpha_{xx} = -(\sigma_{xx}E_x + \sigma_{xy}E_y)/|\nabla T|,$$

$$\alpha_{xy} = (-\sigma_{xy}E_x + \sigma_{xx}E_y)/|\nabla T|. \quad (2)$$

Under field reversal ($\mathbf{H} \rightarrow -\mathbf{H}$), $S$ is symmetric, whereas $S_{yx}$ is antisymmetric. For each curve taken in field, we repeat the measurement with $\mathbf{H}$ reversed. All curves of $S$ and $S_{yx}$ reported here have been (anti)symmetrized with respect to $\mathbf{H}$. As for charge-inversion symmetry, we expect the sign of $S$ to be odd with respect to the shifted gate voltage $V_g' \equiv V_g - V_0$, with $V_0$ the offset voltage ($V_g' = 0$ defines the charge-neutral Dirac point). However, the Nernst signal $S_{yx}$ is symmetric in $V_g'$.

Figure 1(b) shows traces of $S$ vs $V_g$ at selected $T$ with $H = 0$. The thermopower $S$ changes sign as $V_g$ crosses the Dirac point, becoming positive (negative) on the hole (electron) side. The peak value $S_m$ is nominally $T$ linear from $\sim 20$ K to 300 K [Fig. 1(c)].

In sharp contrast to the smooth variation in Fig. 1, the

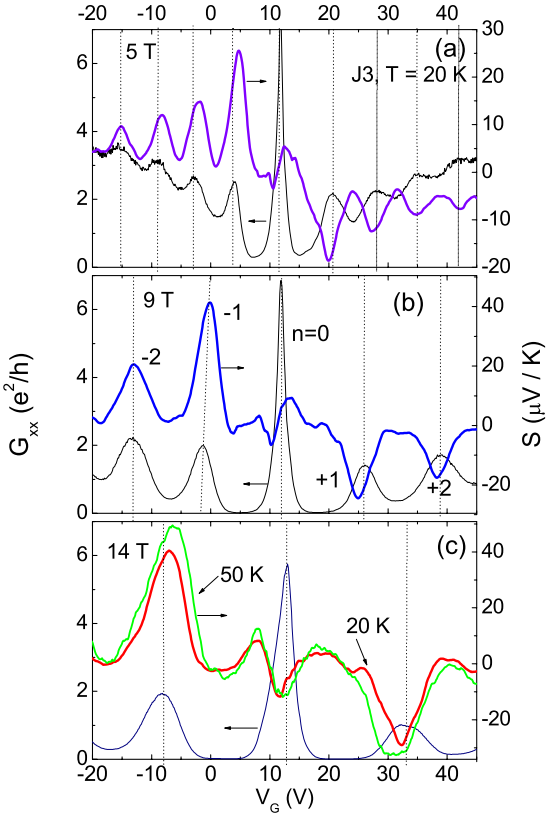


FIG. 2. (Color online) Variation in thermopower $S$ vs $V_g$ (bold curves) and conductance $G_{xx}$ vs $V_g$ (thin curves) in sample J3 at $H = 5$, 9, and 14 T [panels (a), (b), and (c), respectively]. The offset $V_0 = 12.5$ V. All curves were measured at 20 K except for the curve at 50 K in panel (c). Vertical lines locate the maxima of $G_{xx}$. The LL index $n$ is indicated in panel (b).

curves of $S$ vs $V_g$ at finite $H$ show pronounced oscillations, reflecting Landau quantization of the Dirac states. Figures 2(a)–2(c) display $S$ vs $V_g$ (bold curves) with $H$ fixed at the values 5, 9 and 14 T, respectively. For comparison, we have also plotted (as thin curves) the corresponding conductance $G_{xx} = \sigma_{xx}$. [With the exception of the curve at 50 K in panel (c), all curves were measured at 20 K.] Whereas at large $|n|$, the peaks in $S$ are aligned with those in $G_{xx}$ [vertical lines in Fig. 2(a)], at $n = \pm 1$, they disagree. In panel a, the peaks for $V_g' < 0$ (hole doping) decrease systematically in magnitude as $n$ increases from 1 to 4.

In Ref. 8, GJ show that, at each $n \neq 0$, the edge current difference $\delta I_y$ leads to a quantized $\alpha_{yy}$, viz.

$$\alpha_{xy}(\mu) = \frac{k_B e}{h}\beta\int_{E_n}^{\infty} d\epsilon(\epsilon - \mu)\left(-\frac{\partial f}{\partial \epsilon}\right), \quad (3)$$

where $\beta = (k_B T)^{-1}$ and $f(\epsilon)$ is the Fermi-Dirac distribution. As $\mu$ is varied, $\alpha_{xy}$ rises to a narrow peak with peak value $\alpha_{xy}^{\max} = (k_B e/h)\ln 2 \simeq 2.32$ nA/K, attained when $\mu$ equals $E_n$ in the bulk. The width of the peak—discussed below—broadens linearly with $T$.

When combined with $\sigma_{ij}$, Eq. (3) implies that at LL $n$, the thermopower has a peak value

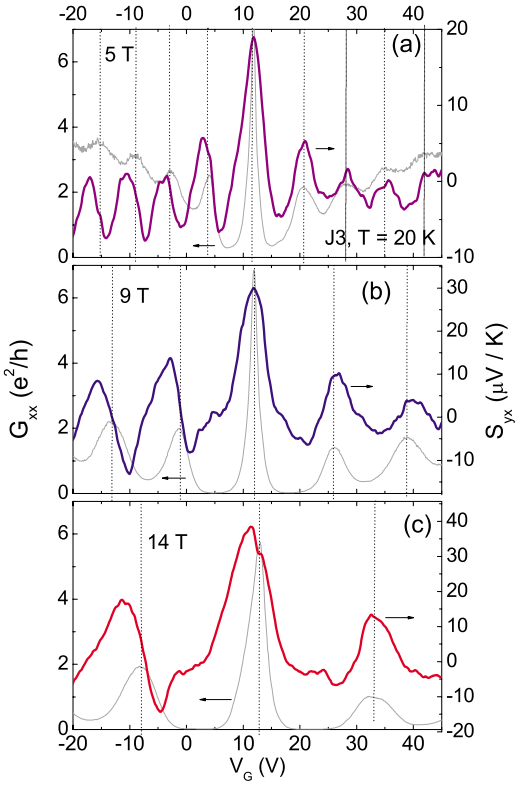


FIG. 3. (Color online) Variation in Nernst signal $S_{yx}$ vs $V_g$ (bold curves) and conductance $G_{xx}$ vs $V_g$ (thin curves) in J3 at the three field values $H=5$, 9, and 14 T [panels (a), (b), and (c), respectively]. All curves were measured at 20 K. Vertical lines locate the maxima of $G_{xx}$. At the Dirac point ($V_g'=0$), the sign of $S_{yx}$ (i.e., $E_y$) is positive, the same as for the vortex-Nernst signal in a superconductor (Refs. 15 and 16).

$$S_{peak}(n) = \frac{k_B}{e}\frac{\ln 2}{\left(n+\frac{1}{2}\right)}. \tag{4}$$

At low $T$, $S$ is independent of $H$ and $T$.

In Fig. 2, the peak value of $S$ at the $n=-1$ LL increases from 25 at 5 T to 41 $\mu$V/K at both 9 and 14 T. Moreover, as $T$ increases from 20 to 50 K (panel c), the peak increases only weakly (41–48 $\mu$V) in sharp contrast with the $T$-linear behavior at $H=0$ (Fig. 1, inset). This is consistent with the prediction of GJ that $S$ (at the peak) saturates to a value independent of $T$ and $H$ at sufficiently low $T$. This saturation contrasts with the $T$-linear behavior of $S$ in $H=0$ [Fig. 1(c)].

In graphene, however, the Berry phase effects lead to a $\frac{1}{2}$-integer shift in the LL index.[3] In evaluating $\sigma_{xy} \sim \Sigma_n f(E_n)$, the $\frac{1}{2}$-integer shift implies that $S_{peak}(n)$ decreases as $k_B \ln 2/(en)$ instead of Eq. (4). The measured values $S_{peak}=41$ $\mu$V/K at $n=-1$ at 9 T already exceeds slightly the predicted value 39.7 $\mu$V/K in Eq. (4). Improved measurements on cleaner samples may yield values closer to the predicted value 59.6 $\mu$V/K for Dirac systems. In principle, Eq. (4) provides a way to measure $\delta T$ on micron-scales with very high resolution—comparable to measurements of resistance.

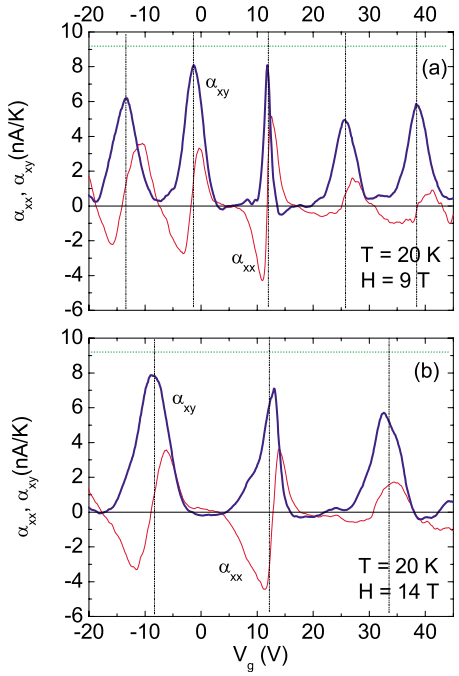


FIG. 4. (Color online) The thermoelectric response functions $\alpha_{xx}$ (faint curve) and $\alpha_{xy}$ (bold) vs $V_g$ at 9 T (a) and 14 T (b) at $T=20$ K calculated from $S$ and $S_{yx}$ [Eq. (2)]. In (a), the width of the peak at $n=0$ is narrower than the others by a factor of $\sim$4. In both panels, vertical lines locate the peaks of $G_{xx}$. The horizontal dashed line is $(4k_Be/h)\ln 2$.

The curves of the Nernst signal $S_{yx}$ are displayed in Fig. 3 for $H=5$, 9, and 14 T. In the three panels, the dominant feature is the large central peak at the $n=0$ LL which towers over the peaks at levels with $n \neq 0$. (By contrast $S$ in Fig. 2 is suppressed at $n=0$ but large for $n \neq 0$.) We note that the observed large Nernst peak and the strong suppression of $S$ at $n=0$ are strongly inconsistent with the flat-top profiles calculated for a system with quadratic dispersion.[9] The positive sign of $S_{yx}$ at $n=0$ implies that the Nernst $E$-field $\mathbf{E}_N$ is parallel to $\mathbf{H}\times(-\nabla T)$ (same sign as in the vortex-Nernst effect in superconductors).[15,16]

With $S$ and $S_{yx}$ measured, we may use Eq. (2) to calculate the thermoelectric conductivity tensor elements $\alpha_{ij}$. We display $\alpha_{xy}$ (bold curves) and $\alpha_{xx}$ (thin curves) vs $V_g$ in Fig. 4(a) (for $H=9$ T) and in Fig. 4(b) (14 T). Unlike $S$ and $S_{yx}$, the peaks in $\alpha_{xy}$ are much narrower and clearly separated by broad intervals in which $\alpha_{xy}$ is nominally zero.

A striking feature of $\alpha_{xy}$ is that its peaks are nominally independent of $n$. The prediction of the model of GJ (Refs. 8 and 9) is that [in the geometry of Fig. 1(a)], the transverse current $J_y$ displays a series of narrow pulses whenever $\mu$ aligns with $E_n$ in the bulk (for $n \neq 0$). The peak current per unit temperature gradient depends only on the combination of universal constants $k_Be/h$. Figure 4 confirms this behavior for $H=9$ and 14 T. The pulses have an average value $\sim$75 nA/K which is within 20% of $(gk_Be/h)\ln 2$ with $g=4$ (horizontal dashed line). Given the large uncertainty in estimating the gradient $-\nabla T$ between the voltage leads, the agreement is satisfactory.

However, the peak of $\alpha_{xy}$ at $n=0$ raises several interesting

questions. As shown in Fig. 1(a), it is not clear how the edge-current calculation of GJ (Refs. 8 and 9) is to be generalized to the $n=0$ LL, which is neither holelike nor electronlike. Hence there is actually no prediction of what the peak value of $\alpha_{xy}$ at $n=0$ should be. Our observation that it also equals $\sim(gk_B/h)\ln 2$ is in need of theoretical explanation.

A bigger puzzle appears when we consider the physical meaning of the area $\mathcal{A}_n(T)$ under each $\alpha_{xy}$ peak. As noted in Eq. (3), the computed profile of $\alpha_{xy}$ vs $\mu$ is a peak whose width increases linearly with $T$. The integral with respect to $\mu$ is readily performed to give $\int d\mu\alpha_{xy}=(c_0 g k_B^2 eT)/h$, independent of $n$ ($c_0\sim 3.29$ is a constant). Noting that $\alpha_{xy}$ in Fig. 4 is plotted vs $V_g\sim n_{2D}$ (the 2D carrier density) rather than $\mu$, we have

$$\mathcal{A}_n(T)=\int dn_{2D}\alpha_{xy}\sim \mathcal{N}_n\frac{c_0 g k_B^2 eT}{h},\quad (n\neq 0), \qquad (5)$$

where $\mathcal{N}_n$ is the peak value of the density of states of the LL of index $n$. At fixed $T$, the area under each peak in Fig. 4 is proportional to $\mathcal{N}_n$.

In Fig. 4, it is quite apparent that the width of $\alpha_{xy}$ at $n=0$ is anomalously narrow by a factor of $\sim 4$ compared with its neighbors. As the peaks attain the same height, the area at $n=0$ is smaller by the same ratio. If we extend Eq. (5) to $n=0$, this implies that $\mathcal{N}_n$ is much smaller for $n=0$ than for $n\neq 0$, which seems unlikely given that states are conserved. The results for $\alpha_{xy}$ uncover a puzzle that resides in the $n=0$ LL$-\alpha_{xy}$ attains a peak value equal to that of its neighbors at $n\neq 0$, but the area enclosed is anomalously small.

These problems underscore further our poor understanding of the $n=0$ LL at the Dirac point. Are the currents carried by edge states for $n=0$? Are there counterpropagating edge states? The thermoelectric response issues are related to problems revealed by resistance experiments. We expect them to be deeply pertinent to the current debate on the nature of the high-field ground state at the Dirac point.[6,7,10–13,17,18]

We are grateful to P. A. Lee for many discussions. The work was supported by NSF through a MRSEC grant (Grant No. DMR-0819860).

[1] K. S. Novoselov, D. Jiang, F. Schedin, T. J. Booth, V. V. Khotkevich, S. V. Morozov, and A. K. Geim, Proc. Natl. Acad. Sci. U.S.A. **102**, 10451 (2005).
[2] K. S. Novoselov, A. K. Geim, S. V. Morozov, D. Jiang, M. I. Katsnelson, I. V. Grigorieva, S. V. Dubonos, and A. A. Firsov, Nature (London) **438**, 197 (2005).
[3] Y. Zhang, J. Tan, H. L. Stormer, and P. Kim, Nature (London) **438**, 201 (2005).
[4] Y. Zhang, Z. Jiang, J. P. Small, M. S. Purewal, Y.-W. Tan, M. Fazlollahi, J. D. Chudow, J. A. Jaszczak, H. L. Stormer, and P. Kim, Phys. Rev. Lett. **96**, 136806 (2006).
[5] Z. Jiang, Y. Zhang, H. L. Stormer, and P. Kim, Phys. Rev. Lett. **99**, 106802 (2007).
[6] J. G. Checkelsky, L. Li, and N. P. Ong, Phys. Rev. Lett. **100**, 206801 (2008).
[7] J. G. Checkelsky, L. Li, and N. P. Ong, Phys. Rev. B **79**, 115434 (2009).
[8] S. M. Girvin and M. Jonson, J. Phys. C **15**, L1147 (1982).
[9] M. Jonson and S. M. Girvin, Phys. Rev. B **29**, 1939 (1984).
[10] H. A. Fertig and L. Brey, Phys. Rev. Lett. **97**, 116805 (2006).
[11] D. A. Abanin, P. A. Lee, and L. S. Levitov, Phys. Rev. Lett. **96**, 176803 (2006).
[12] D. A. Abanin, K. S. Novoselov, U. Zeitler, P. A. Lee, A. K. Geim, and L. S. Levitov, Phys. Rev. Lett. **98**, 196806 (2007).
[13] E. Shimshoni, H. A. Fertig, and G. V. Pai, Phys. Rev. Lett. **102**, 206408 (2009).
[14] J. P. Small, K. M. Perez, and P. Kim, Phys. Rev. Lett. **91**, 256801 (2003).
[15] Y. Wang, L. Li, and N. P. Ong, Phys. Rev. B **73**, 024510 (2006).
[16] In our view, the sign reported in Refs. 17 and 18 is incorrect.
[17] Y. M. Zuev, W. Chang, and P. Kim, Phys. Rev. Lett. **102**, 096807 (2009).
[18] P. Wei, W. Bao, Y. Pu, C. N. Lau, and J. Shi, Phys. Rev. Lett. **102**, 166808 (2009).